La mer 48 : 71-86, 2010
Société franco-japonaise d'océanographie, Tokyo

Development of Algorithms for Estimating the Seasonal Nitrate Profiles in the Upper Water Column of The Sagami Bay, Japan

Andreas A. HUTAHAEAN[1, 6], Joji ISHIZAKA[2*], Akihiko MORIMOTO[2], Jota KANDA[3], Naho HORIMOTO[3], and Toshiro SAINO[4,5]

Abstract: We propose a method to estimate nitrate (NO_3^-) profiles in the upper water column of the Sagami Bay, Japan, using surrogate oceanographic data such as temperature, salinity and chlorophyll *a* (Chl *a*) . Analysis of a 10 year (June 1999-November 2008) dataset revealed that variations in nitrate profiles were associated with seasonal variations of water column structure in the upper 200m of the Sagami Bay. The upper 200m water column structure could be separated into three layers; the surface mixed layer, the intermediate layer, and the deeper layer. The surface mixed layer showed distinct seasonal variability in depth, while the deeper layer than $\sigma_\theta = 26$, located at depths between 130-160m, showed little seasonal variability. Warm and less saline water in the surface mixed layer and the upper intermediate layer during summer and fall indicated that this water was influenced by seasonal heating and freshwater input, and the large variation at these depths indicated the spatial heterogeneity of the water. When the seasonal variability of nitrate and its predictor variables was taken into account, nitrate concentrations in the upper two layers could be reproduced for each season on the basis of temperature and Chl *a*. In the deeper layer, nitrate could be explained without seasonal classification on the basis of temperature and salinity. The empirical algorithms for nitrate in the three layers were used to construct nitrate profiles for four seasons in the Sagami Bay. When the performance of the algorithm was tested against an independent data set, the coefficient of determination and root mean square difference between measured and estimated nitrate in each season ranged between 0.92～0.98 and 1.3～1.6 μM, respectively.To our knowledge, this is the first study that demonstrates that nitrate profiles in the upper 200m coastal oceanic waters can be reproduced based on temperature, salinity and Chl *a* data. These latter datasets are now routinely measured on various platforms, such as ships, floats, gliders, and buoys, using CTD and Chl *a* sensors and hence these algorithms could greatly aid in biogeochemical cycle studies in the oceanic environments, especially in highly dynamic coastal regions.

Keywords: *nitrate algorithm, mixed layer depth, water mass, Sagami Bay-Japan.*

1. Graduate School of Environmental Studies, Dept. of Earth & Environmental Sciences, Nagoya University, Japan.
2. Hydrospheric and Atmospheric Research Center (HyARC), Nagoya University, Japan.
3. Dept. of Ocean Sciences, Tokyo University of Marine Science and Technology, Japan
4. Research Institute for Global Change (RIGC) , Japan Agency for Marine-Earth Sciences and Technology (JAMSTEC), Yokosuka, Japan.
5. Japan Science and Technology Agency (JST), Kawaguchi, Japan.
6. Agency for Marine and Fisheries Research (BRKP-WILNON) , Jakarta, Indonesia.

* *Corresponding author*
Email: jishizak@hyarc.nagoya-u.ac.jp
Address: Hydrospheric Atmospheric Research Center (HyARC), Nagoya University
Furo-cho, Chikusa-ku, Nagoya 464-8601, Japan.

1. Introduction

Light and nutrients are major factors controlling phytoplankton growth in the upper layer of the ocean (PARSONS *et al.*, 1977; ARRIGO, 2005). Nitrate (NO_3^-) in particular is important because it is a main source of nitrogen supporting new production (DUGDALE and GOERING, 1967) and because in general in many of the world's oceans, phytoplankton biomass in the upper water column is strongly regulated by nitrate availability (FANNING, 1989; LEVITUS *et al.*, 1993). The availability of nitrate in the euphotic zone is strongly regulated by vertical mixing and advective supply of nitrate to the upper euphotic layers of the ocean, both of which in turn are influenced by variations of environmental forcing, such as solar heating, wind stress, and/or intrusion of different water masses (PRICE *et al.*, 1986; MARRA *et al.*, 1990). Despite its importance, quantitative estimates of nitrate concentrations are limited because of the logistical difficulties in measuring nitrate temporally and spatially by conventional ship observations. There have been attempts to estimate nitrate by automated nitrate sensors on moorings or profiling floats (JOHNSON *et al.*, 2006), but limitations in sensor availability have been a major impediment to these measurements becoming routine.

Previous studies showed a strong negative correlation between temperature and nitrate, a reflection of the processes of nutrient supply from the deep into the mixed layer (KAMYKOWSKI, 1987; GARSIDE and GARSIDE, 1995). This correlation has been used in a number of recent studies for estimating nitrate concentrations in surface water using remotely sensed sea surface temperature (SST) (KAMYKOWSKI and ZENTARA, 1986; GARSIDE and GARSIDE, 1995; GONG *et al.*, 1995; KAMYKOWSKI *et al.*, 2002; SWITZER *et al.*, 2003). The use of temperature alone as a surrogate to estimate nitrate is, however, limited in areas where phytoplankton activity is high (GOES *et al.*, 1999; 2000). This is especially true in high to mid latitude regions, where short lived bursts of phytoplankton growth, such as during spring or during bloom formation, can have a strong influence on nitrate availability. To account for biological activity, GOES *et al.* (1999, 2000) proposed the use of chlorophyll *a* (Chl *a*) as an additional determinants of nitrate, and showed that its addition could greatly improve the nitrate estimation in the surface ocean.

Since the empirical algorithms of GOES et al, (1999, 2000) were meant for use with satellite data, they were limited to the surface and relied primarily on satellite derived fields of SST and Chl *a*. Here we describe an approach to estimate nitrate concentration from the surface to the ocean's interior (200 m depth). The method uses temperature, Chl *a* and salinity as predictor variables to estimate nitrate concentration not only in the surface but also in the subsurface layer (e.g. below euphotic zone) of water column. We show that the algorithms, when applied to CTD and Chl *a* data that are now routinely derived from moorings and profiling platforms, can be extremely useful to understand nitrate variability in highly dynamic coastal environments, such as the Sagami Bay. The bay is situated on the east coast of Honshu Island, Japan and in a region that comes under the influence of several source waters including the Kuroshio current water.

2. Methods and Data

2.1 Study Site

Sagami Bay, located in the southeastern part of Honshu Island, Japan, has a wide mouth open toward the Pacific Ocean (Fig. 1A). The water in the bay is influenced by both the Kuroshio current water and the coastal waters. IWATA (1985) and more recently HINATA *et al.* (2005) found that the offshore water between the Kuroshio front and Honshu Island, which originates outside of the bay, influences surface water in the bay. Intermediate Oyashio water, which has low temperature (<7.0℃), low salinity (34.2) and high dissolved oxygen concentration (>3.5 ml l^{-1}), sometimes intrudes into the bay at depth along the isopycnal surface of $\sigma_\theta = 26.8$ (SENJYU *et al.*, 1998). The water in the bay also frequently exchanges with both Tokyo Bay and Pacific Ocean as observed by YANAGI and HINATA (2004).

2.2 Data Sources

Development of the empirical algorithms was

Table 1. Data sources for constructing the nitrate algorithms

No	Data Sources	Cruises / Date	Number of Profiles
1	*T/V* Seiyo Maru	Monthly Time Series (June 1999–Sept 2007) except: Oct 1999; Nov 2001; Jan–Feb 2002; Jan 2004	95
2	*R/V* Tansei Maru	a. 2004	12
		- KT 04–04 (23–25 April)	7
		- KT 04–11 (8–12 June)	7
		- KT 04–15 (31 July–2 Aug)	
		b. 2006	13
		- KT 06–08 (2–4 May)	
		c. 2007	4
		- KT 07–10 (18–20 May)	28
		- KT 07–17 (19–26 July)	23
		- KT 07–30 (13–20 Nov)	
		d. 2008	8
		- KT 08–01 (20–23 Feb)	10
		- KT 08–05 (1–7 April)	22
		- KT 08–15 (6–10 July)	21
		- KT 08–24 (23–27 Sept)	6
		- KT 08–29 (6–10 Nov)	
3	JODC	September, 1996	6

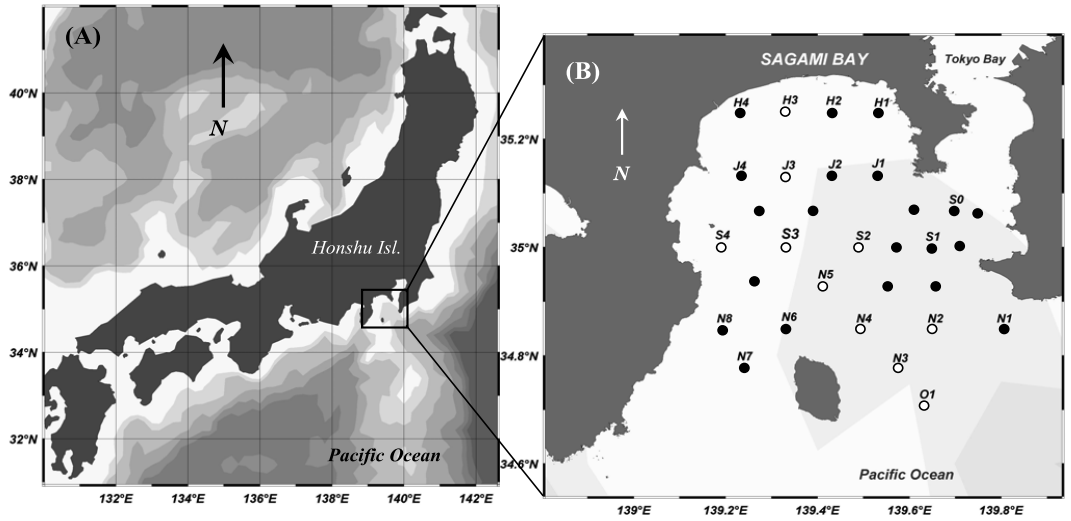

Fig. 1. Maps of Japan (A) and Sagami Bay (B) with the sampling stations of nitrate, CTD and Chl *a*. Stations indicated by white circles represent the sampling points of independent data sets used for the algorithm validation.

undertaken using temperature, salinity, nitrate and Chl *a* from surface to 200m depths from the following data sources (Table 1) : (1) long term monthly cruises from 1999-2007 at Stn. S3 by *T/V* Seiyo Maru of Tokyo University of Marine Science and Technology, (2) cruises carried out by Nagoya University by using *R/V* Tansei Maru for collecting data at many stations in the entire bay, and (3) Japan Oceanographic Data Center (JODC). A fraction of the data from (2), not used for constructing the algorithm, was used as independent data set to test the performance of the algorithms that were generated (Table 2,

Table 2. Independent data sources for testing the algorithms performance.

No	Cruise	Stations	Number of Profiles	Seasons
1	KT08–01	S3, H3, J3, N5	4	Winter
2	KT08–05	S3, N3, N4, J3, H3, O1	6	Spring
3	KT08–15	H3, J3, N3, S3	4	Summer
4	KT07–30		6	Fall
	KT08–29	S3, H3, J3, N3, N4, N5		

Fig. 1B).

During cruises (1) and (2), seawater samples were collected with 5 or 10L Niskin samplers mounted as a rosette around a CTD (I-CTD and NXIC-CTD, Falmouth Scientific-INC). Samples for nitrate and Chl *a* were collected at discrete depths in the water column from the surface (5m or 10m) to 200 m water depths. Sampling depths were not always consistent for each cruise. Samples for nitrate were stored in polystyrene bottles, frozen immediately after the collection and stored at −20℃ until analysis. Nitrate concentrations in water sample collected by *T/V* Saiyo Maru and *R/V* Tansei Maru were measured by auto-analyzers AACS III and TRAACS 2000 (Bran and Luebbe), respectively (HASHIMOTO *et al.*, 2005). Chl *a* in samples were measured by filtering 200 ml water samples onto 25 mm Whatman GF/F filters. Chl *a* was immediately extracted by immersing the filter into *N, N*-dimethylformamide (SUZUKI and ISHIMARU, 1990) under cold and dark conditions, for at least 24 hours prior to the analysis. Chl *a* concentrations were determined using a Turner Design Model 10-AU fluorometer calibrated with standard Chl *a* (Wako Pure Chemical Industries), according to the method of WELSCHMEYER (1994).

2.3. Data Analysis

The database used for constructing the algorithms for nitrate yielded 262 profiles of temperature, salinity, nitrate and Chl *a* in the upper 200m layer. Nitrate and Chl *a* profiles consists of 8–12 sampling depth points, which varied among the different cruises, while temperature and salinity profiles were measured continuously by using a CTD and used for deriving water density gradients. The total number of data points containing temperature, salinity, Chl *a* and NO_3^- was 3324. The mixed layer depth (MLD) was established based on a difference in water density of 0.125 from the surface layer (LEVITUS, 1982). The data from the long term monthly cruises at Stn. S3 by *T/V* Seiyo Maru were used for the analysis of seasonal variability.

Relationship between nitrate concentration and its predictor variables were analyzed by multiple linear regression analysis. The predictive accuracy of the regression model was characterized using root mean square error (RMSE) with data numbe of *N* (KAMYKOWSKI *et al.*, 1986; GARSIDE and GARSIDE, 1995; GOES *et al.*, 1999 and 2000; SWITZER *et al.*, 2003);

$$RMSE = \sqrt{\frac{1}{N}\sum_{i=1}^{N}(NO_{3estimated} - NO_{3measured})^2}, \quad (1)$$

where $NO_{3estimated}$, and $NO_{3measured}$ is estimated and measured nitrate concentration (μM) for sample *i*, respectively.

3. Results

3.1. Water Column Structure of the Upper 200 m of Sagami Bay.

As shown in the T-S diagram from the archived data of Sagami Bay (Fig. 2A), the temperature and salinity ranged from 8.9–28.5℃ and 32.1–34.7, respectively. It is clearly seen that the denser deeper water showed less variability in temperature and salinity compared to the less dense upper water column waters. Figs. 2B-E show the seasonal variability associated with Fig. 2A, indicating that the higher temperature and less saline shallow waters in summer and fall. It is important to note that the denser water (σ_θ>24.3) had little variability in salinity and fell onto a line on the T-S diagrams (Figs. 2A-E), particularly below the water with σ_θ of 26. This σ_θ of 24.3 and 26 also nearly corresponded to the density of the surface water during winter and spring and

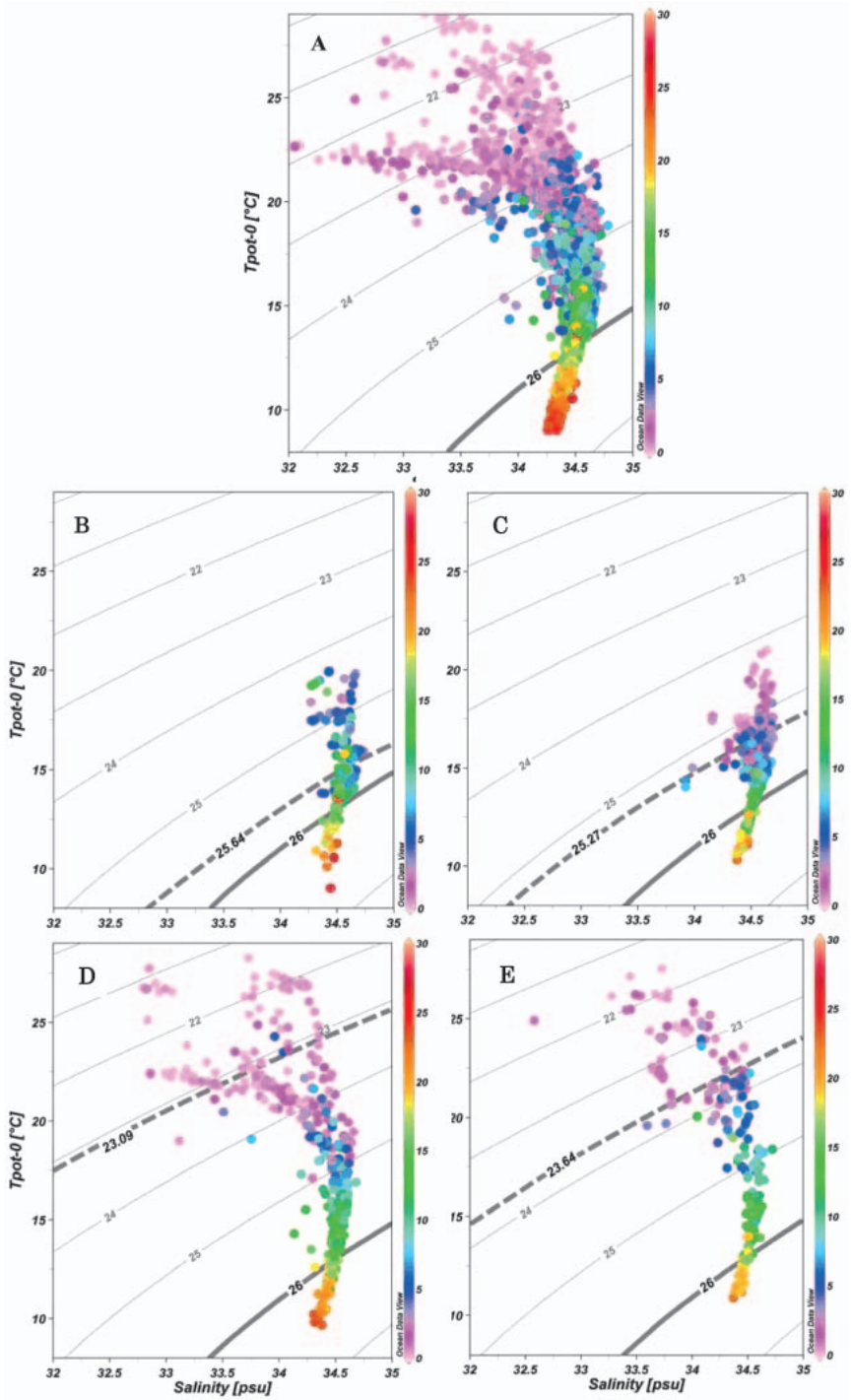

Fig. 2. The T-S diagrams of the upper 200m waters in Sagami Bay for all seasons (A), winter (B), spring (C), summer (D) and fall (E). The color bar represents nitrate concentration (μM). The thick lines correspond to the $\sigma_\theta = 26$ isopycnal surface and the thick dotted line shows the average water density of MLD waters in each season.

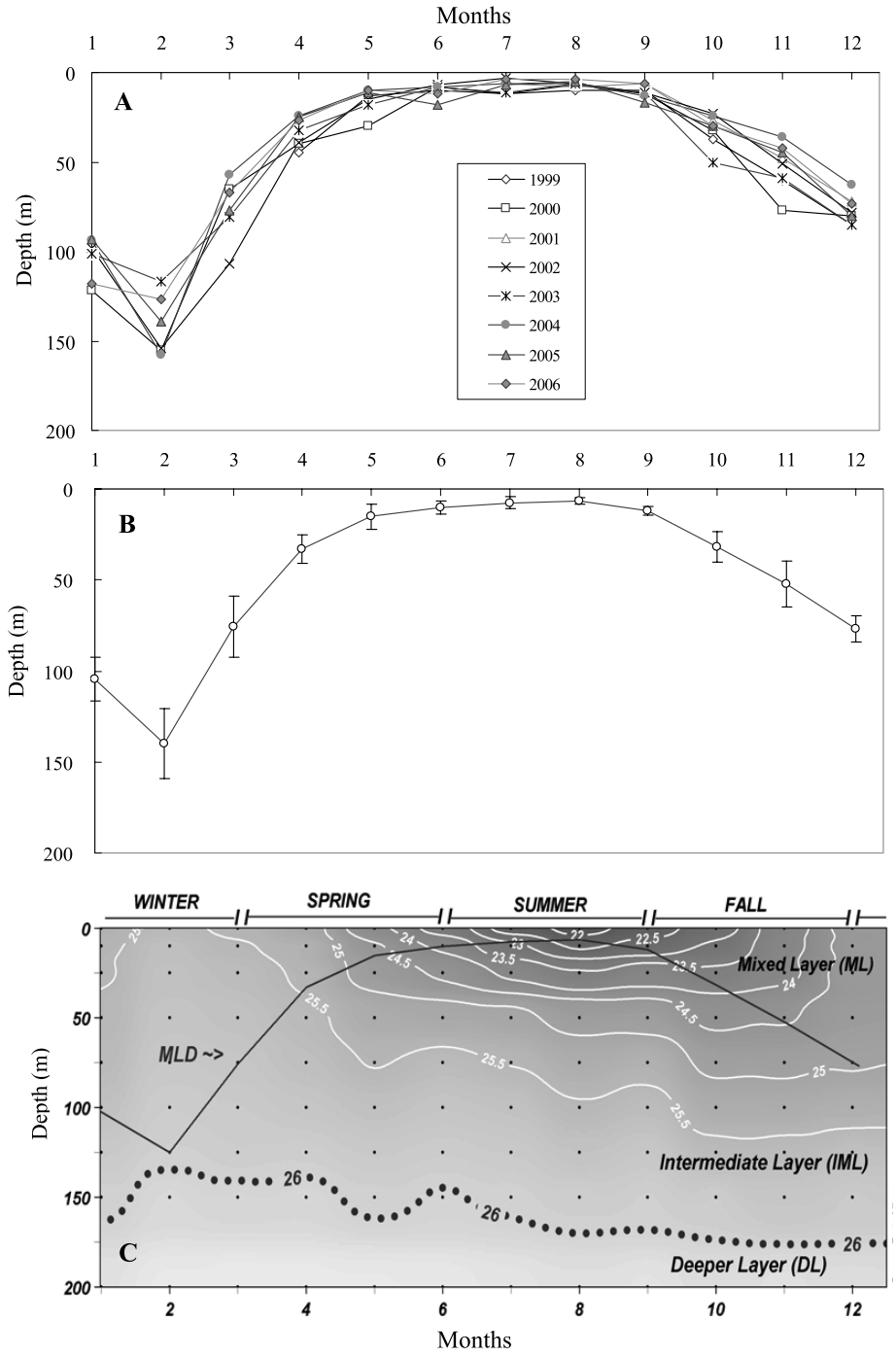

Fig. 3. Seasonal variation of mixed layer depth (A) and the average with standard deviation (B) at stn. S3 in Sagami Bay from 1999 to 2006. Seasonal density structure of the upper 200m water column of Stn. S3 (C). Dot and solid lines indicate $\sigma_\theta = 26$ and bottom of the mixed layer, respectively. The top layer is named as mixed layer (ML), and the second layer is the intermediate layer (IML), and the last layer is the deeper layer (DL).

Table 3. Correlation coefficient (r) between nitrate and its predictor variables in mixed layer water, intermediate water, and deeper water. n is number of data points.

NO	Predictors	Winter	Spring	Summer	Fall
Mixed Layer		n=212	n=215	n=87	n=242
1	Temperature	-0.49**	-0.68**	-0.35*	-0.91**
2	LogTemperature	-0.49**	-0.68**	-0.36*	-0.91**
3	Chlorophyll*a*	0.45**	0.51**	0.17	0.68**
4	Salinity	0.07	0.01	0.03	0.49**
Intermediate Layer		n=222	n=255	n=1183	n=243
5	Temperature	-0.71**	-0.86**	-0.94**	-0.93**
6	Log Temperature	-0.71**	-0.85**	-0.95**	-0.93**
7	Chlorophyll *a*	0.69**	0.48**	0.48**	0.63**
8	Salinity	0.69**	0.45**	0.24	0.23
Deeper Layer		n=665			
9	Temperature	-0.87**			
10	Log Temperature	-0.87**			
11	Chlorophyll *a*	0.05			
12	Salinity	0.85**			

** $p < 0.001$; * $p < 0.05$

bottom of the winter mixed layer, respectively. The shallow warm and less saline water in summer and fall was in probability generated by both heating and freshwater supply in the bay as well as lateral transport from outside of the bay.

Fig. 3 shows seasonal variability of the depth of the surface mixed layer in the central part (Stn. S3) of the Sagami Bay. The seasonal variability of each year from 1999 to 2006 shows that the mixed layer depth (MLD) was deepest in February, shoaled rapidly in March and April, became shallowest in summer months (June to August), and then gradually deepened from September to February (Fig. 3A). The deepest MLD in February, varied from year to year, ranging from 115 m in 2003 to 160 m in 2004 (Figs. 3A-C). On the basis of the seasonal variability of the averaged MLD (Fig. 3B), each year can be classified into four seasons with regard to seasonal evolution of the MLD as depicted in Fig. 3C; (a) winter (December to February) when the MLD became deeper due to intensive cooling, (b) spring (March to May) when the MLD became shallower due to heating, (c) summer (June to August) when the MLD were very shallow and closed to the surface, and (d) fall (September to November) when the MLD started to deepen due to gradual cooling. As is evident from Fig. 2, the deeper water (σ_θ>26) in Sagami Bay showed little variability in the T-S diagram. The depth corresponding to 26 σ_θ was ca. 130-160 m in Sagami Bay at Stn. S3 with little seasonal variability (Fig. 3C). Based on the seasonal variability of the ML and the depth of σ_θ = 26, we classified the upper 200 m water column of the Sagami Bay into 3 layers; (1) the mixed layer (ML) above the MLD, (2) the intermediate layer (IML) below the MLD and above the depth of σ_θ = 26, and (3) the deeper layer (DL) with σ_θ > 26.

3.2 Development of Nitrate Algorithms

Of the 262 profiles available from the dataset used in this study, 104 profiles were taken in summer and the rest during the other seasons. Also of the 262 profiles, 45 profiles were from Stn. S3. The number of profiles was smallest in winter with 29 profiles (10.9 % data points) of which more than 2/3 (20 profiles) were from Stn. S3. In spring and fall there were 50 profiles (17.5% data points) and 79 profiles (20.7% data points), respectively. The seasonal unevenness in the number of profiles apparently resulted from the observations out of the Stn.S3 during R/V Tansei Maru cruises in summer and fall. Number of profiles at Stn. S3 showed less seasonal bias. As for the spatial distribution of the data set, almost half of the data were obtained at Stn. S3 (～45.1%), but other 9 stations distributed evenly in the bay (Fig. 1B). The frequency distribution of data numbers in 3 different waters classified in section 3.1 shows

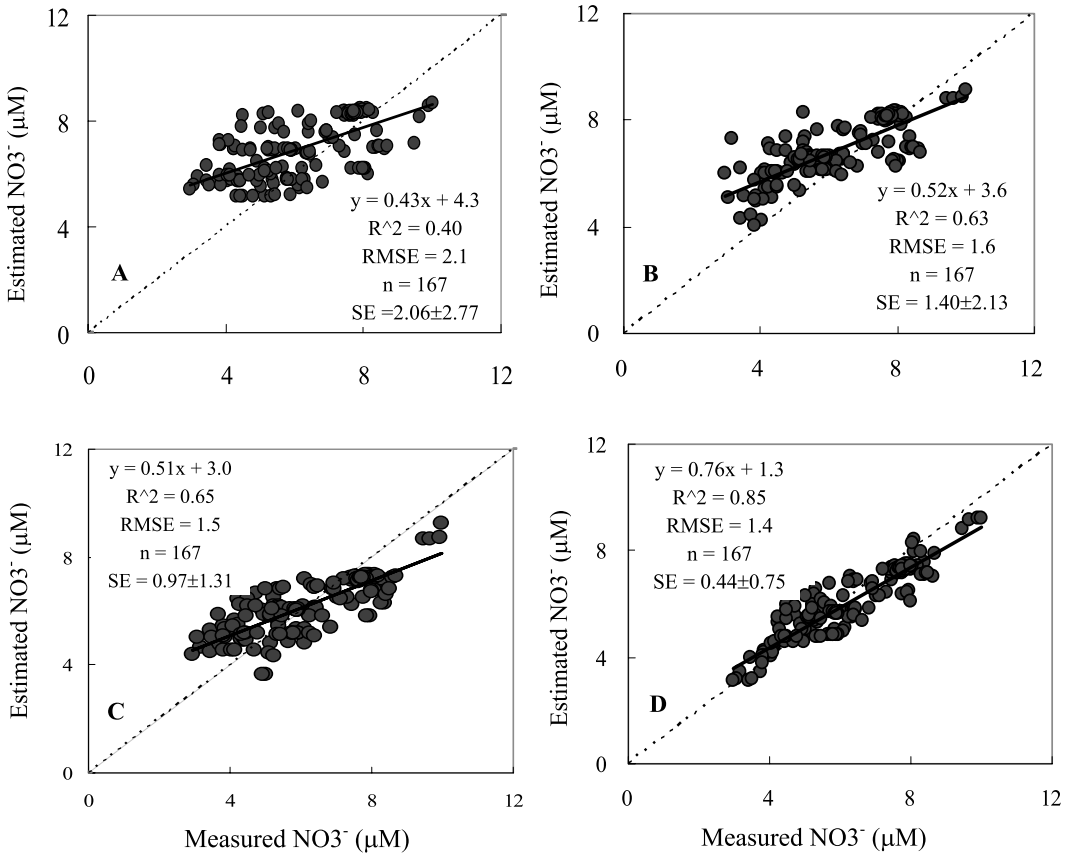

Fig. 4. Relationship between measured and estimated nitrate concentrations in ML as an example of processes in developing the nitrate algorithms: (A) Linear regression with temperature, (B) Multiple linear regression with temperature and Chl *a*, (C) Multiple linear regression with Log T and Chl *a*, and (D) Multiple linear regression with temperature, Log T and Chl *a*. RMSE and SE indicate Root Mean Square Error and Standard Error with the standard deviation, respectively.

about 57.2% (1903 points) of data points were obtained from the IML, with highest number of 1183 points found in summer. On the other hand, data from ML and DL consisted of 22.8% and 20%, respectively. This vertical distribution showed that the database was more concentrated at IML than other waters.

Table 3 shows the correlations between measured nitrate concentration and each possible predictor variable in different water masses and seasons. For the most cases within the ML and the IML, temperature, the logarithm of temperature (Log T), and Chl *a* correlated significantly with nitrate. In contrast, high correlation was observed for the DL nitrate with temperature and salinity. The large difference in temperature within the water column, between the surface ML and DL, required the conversion of temperature to Log T to reduce the variability in GOES *et al.* (1999; 2000), SILIÓ-CALZADA *et al.* (2008) and STEINHOFF *et al.* (2009) independently showed that the addition of the Log T improved NO_3^- prediction by multiple-linear regression.

An example of the improved relationship between nitrate concentration in the ML and its predictor variables with additional variable is shown in Fig. 4. Addition of Chl *a* and the use of Log T both improved the predictability of the model compared to the regression with temperature alone (Figs. 4A and 4B). Furthermore, the combination of temperature, Chl *a*

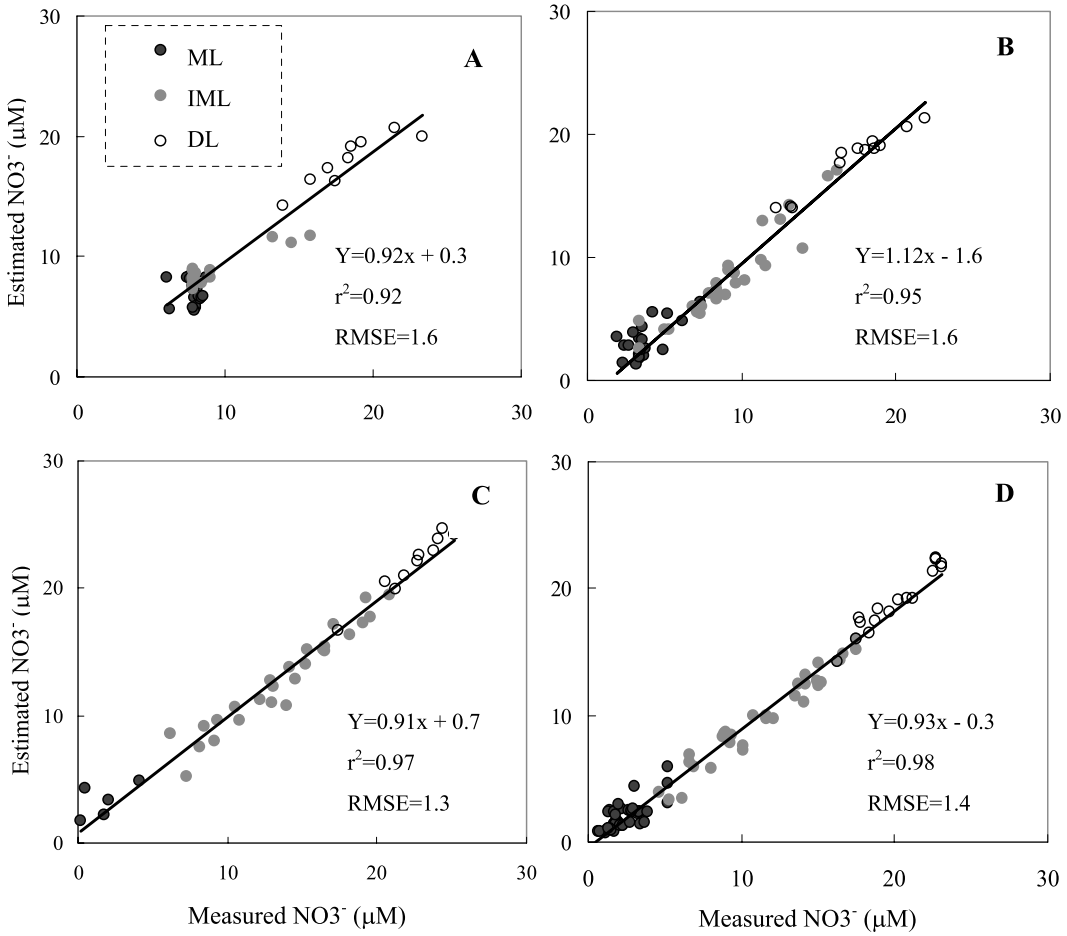

Fig. 5. Regressions of measured and estimated nitrate concentrations using independent data sets obtained in Sagami Bay from locations shown in Figure 1B in winter (A), spring (B), summer (C) and fall (D).

and Log T significantly improved the predictability (Figs. 4C and 4D). Hereafter, we used multiple-linear regression analysis of nitrate with temperature, Log T and Chl *a* for the ML and the IML season by season, and for DL with temperature, Log T and salinity.

Nitrate concentration in each season was estimated by applying the above algorithms to ML and IML (Eq. 2) and DL (Eq. 3), respectively.

$$\text{Nitrate}\ [\mu M] = a + b\ T\ [\text{deg C}] + c\ \text{Chl}\ a\ [\mu g\ l^{-1}] + e\ \log T\ [\text{deg C}] \quad (2)$$

$$\text{Nitrate}\ [\mu M] = a + b\ T\ [\text{deg C}] + d\ \text{Sal}\ [\text{psu}] + e\ \log T\ [\text{deg C}] \quad (3)$$

Results of multiple-linear regression to estimate nitrate concentration are shown in Table 4. The r^2 ranged from 0.59 to 0.93, and RMSE from 0.6 to 2.1 μM. It is notable that the lowest r^2 of 0.59 and the second smallest RMSE of 0.7 μM were observed in the summer ML, where the data number was smallest and the nitrate concentration was the lowest. Except for the summer, r^2 values during the other seasons were larger than 0.73.

3.3. Applicability of the Regression Models

A set of independent data (Table 2) from several stations obtained during the *R/V* Tansei Maru cruises (Fig. 1B) was used to test the performance of the nitrate algorithms. The

NO_3^- profiles in the upper 200 m water column of the Sagami Bay were computed by using a combination of multiple-regression models for the three layers described in the previous section, and the correlations between measured and estimated nitrate are shown in Fig. 5. The highest performance of the algorithms was observed in fall with r^2 and RMSE of 0.98 and 1.4 μM, respectively. On the other hand, the lowest performance was found during winter with r^2 and RMSE of 0.92 and 1.6 μM, respectively. In spring and summer the algorithm results in r^2 and RMSE of 0.95 and 1.6 μM, 0.97 and 1.3 μM, respectively.

4. Discussion

4.1. Water Mass and Nitrate Variability in Sagami Bay

Our analysis of T-S diagrams (Fig. 2) revealed conspicuous seasonal variations of water mass. The largest variability in the T-S diagram was observed during summer and fall in the surface mixed layer. This high temperature and less saline water mass appeared on the top of the winter low temperature and high saline water mass. The water mass with density of σ_θ >24.3, and more specifically σ_θ >26, showed very stable T-S signatures for all seasons during the 10 years. This may suggest that this water mass came from same source during all seasons. This water mass was at surface in winter and spring and below the surface water in summer and fall.

The high temperature and less saline surface water appeared in summer to fall and showed large variability in their T-S signatures. Like any other temperate region, radiation flux increases during summer and peaks in July (HASHIMOTO *et al.*, 2005; 2006; ISHIZAKA *et al.*, 2007), and high heat flux in summer affects the heat content in the upper water column of the Sagami Bay and changes the water properties (OTOBE and ASAI, 1985). Freshwater input from river and lateral transport of less saline water from Tokyo Bay can also influence the surface water of Sagami Bay, specifically during summer (KANDA *et al.*, 2003; YANAGI and HINATA, 2004). The variability of T-S diagram at the surface indicated the heterogeneity of the less saline water in summer. Those dynamics of the water mass in the Sagami Bay was fairly consistent with the one described previously (IWATA, 1985) and similar to the near-by Suruga Bay (NAKAMURA, 1982 referred in IWATA *et al.*, 2005).

It is known that the vertical mixing and the upward transport of nutrients in Sagami Bay during the summer stratified season takes place due to physical forcing, such as regional upwelling (KAMATANI *et al.*, 1981), topographic effect on strong current (TAKAHASHI *et al.*, 1980), and wind (ATKINSON *et al.*, 1982). In most cases, these vertical mixing and upwelling events cause relaxation of the seasonal thermocline resulting in mixing in the upper water column < ～100m and/or upwelling of deeper water to the upper water. These events may be responsible for the large variability of surface T-S diagram during the summer and fall.

Previous studies (BAEK *et al.*, 2009; TAKAHASHI *et al.*, 1986) have shown that riverine inputs and mixing/upwelling can lead to significant increases in the amount of nitrate in the bay. However, in our dataset, nitrate concentrations in the surface mixed layer in summer were usually low (0.1–1.6 μM), despite indications of large riverine inputs and upwelling as evident from the variability at the surface in the T-S diagram during summer. One possibility is that nitrate increases due to these sporadic events was quickly consumed by phytoplankton and depleted. On the basis of experimental data and field-observations, ISHIZAKA *et al.* (1983) and TAKAHASHI *et al.* (1986) showed that excess nitrate present in upwelling water in the Sagami Bay was rapidly depleted by fast growing phytoplankton to limiting concentrations. Satellite data showing large heterogeneity of Chl *a* and primary production in the bay provides an indication of the rapid response of phytoplankton to these events and the variability in nitrate associated with phytoplankton biomass distribution (ISHIZAKA *et al.*, 1992; 2007; KANDA *et al.*, 2003). These observations justify the importance of inclusion of Chl *a* in the nitrate algorithm.

The lack of seasonal variability in the T-S diagram (Fig. 2) for waters below the depth of

$\sigma_\theta = 26$, between 130 and 160 m, suggested minimal influence of lateral advection on nitrate distribution. Furthermore, it suggested that the DL was stable in the entire region of the Sagami Bay at least during the observation period. This was an unexpected finding because the Sagami Bay is located close to the Kuroshio and hence its water mass structure is believed to be affected by its dynamical forcing (YANAGI and HINATA, 2004; HINATA *et al.*, 2005). It has also been reported that the Oyashio water sometimes intrudes into Sagami Bay in much deeper layer (～300m; SENJYU *et al,* 1998). Since our observations were limited to 200m, we do not know much about the depth range of the stable water mass below this depth.

Nitrate concentration in the DL were strongly correlated with temperature and salinity but not with Chl *a*. This is not an unexpected finding as phytoplankton photosynthetic activity and nutrient uptake in deeper waters would have been minimal as is also evident from the extremely low Chl *a* concentration in the DL (<0.07 μg l^{-1}) compared to the ML (0.03–7.12 μg l^{-1}) and the IML (0.01–4.16 μg l^{-1}).

In the present study, we defined the IML as the water mass below the ML and above the DL. It was very thin during winter/spring and thick during summer/fall because of the deep and shallow ML, respectively. The T-S diagrams (Figs. 2B-C) show that the ranges of σ_θ in IML were narrower, 25.6–26 and 25.3–26, in winter and spring and but were broader, 23.1–26 and 23.6–26, in summer and fall, respectively. This broader range in σ_θ, in the IML, can be attributed to mixing of the warm and less saline summer-time surface water with waters in the upper part of the IML. The large amount of phytoplankton in the upper part of IML, which was invariably shallower than the euphotic zone (～30–67 m, HASHIMOTO *et al.*, 2006) during summer, justified the inclusion of Chl *a* as a predictor variable in the multiple-linear regression of nitrate concentration in the IML.

4.2. Nitrate Algorithm: Strength and Limitations

Our data set revealed that nitrate concentration could be estimated with a great degree of reliability using temperature and Chl *a* in the ML as well as in the IML. In the DL, nitrate correlated well with temperature and salinity (Table 3). This is an important finding not only for explaining what regulates NO_3 variability in the bay, but also for explaining the rationale in our choice of variables for the algorithms for different depths.

There have been previous attempts to estimate nitrate from the temperature, salinity and Chl *a*. GOES *et al.* (1999; 2000) and SILIÓ-CALZADA *et al.* (2008) showed that variability of nitrate at the surface could be explained by SST and Chl *a* in the Pacific Ocean and in the Benguela Upwelling, respectively. GARSIDE and GARSIDE (1995) and GARSIDE *et al.* (1996) were able to explain the variability of nitrate and its origin on the basis of temperature for deep water in the Equatorial Pacific and coastal water of the Gulf of Maine and salinity, respectively. IWATA *et al.* (2005) used salinity alone for estimating subsurface nutrient in Suruga Bay, Japan.

In this study, nitrate profile from surface to 200m could be estimated using different algorithms for different layers of vertical structure taking into account not only different physical and biological processes but the origins and mixing of different source waters. The estimation of accurate vertical profile of nitrate was not possible by other methods, and the present algorithms should be helpful for understanding the biogeochemical processes in dynamical marine environments such as the Sagami Bay.

In general, the algorithms performed better in the IML and in the DL than in the ML (Table 4). One of the reasons for this discrepancy may be the highly dynamic nature of the ML with large variability in temperature, salinity, and Chl *a*, but a small range of variability in nitrate, particularly during summer. In the ML, the weakest correlations between measured and estimated nitrate were found in summer. This is perhaps due to the low nitrate concentrations observed, but also because of the large variability of temperature as

Table 4. Results of multiple linear regressions for estimating nitrate concentration. N is number of data. The values of a, b, c, d and e are constant and coefficients of equation for mixed layer water and intermediate water (eq. 2) and for deeper water (eq.3)

No Seasons	Constant	T	Chl a	Sal	Log T	R^2	RMSE (μM)	N
	a	b	c	d	e			
Mixed Layer								
1 Winter	145.57	3.27**	3.41**	----	-68.32*	0.73	1.4	212
2 Spring	95.51	0.85**	1.81**	----	-93.44*	0.78	1.9	215
3 Summer	212.7	0.85*	0.30*	----	-37.08*	0.59	0.7	87
4 Fall	22.12	-1.51**	2.41**	----	3.58**	0.92	1.2	242
Intermediate Layer								
5 Winter	329.52	11.5**	-5.92**	----	-181.02**	0.76	2.1	222
6 Spring	187.85	3.68**	-1.77*	----	-86.59**	0.83	1.8	255
7 Summer	83.88	-0.15**	-0.12*	----	-25.76**	0.93	0.6	1183
8 Fall	98.76	0.92**	-3.72**	----	-36.71**	0.88	1.8	243
Deeper Layer								
9 All Seasons	416.33	2.01**	---	11.00**	2.01**	0.90	0.6	665

** P<0.001; * P<0.05

compared to other seasons.

For the development of the algorithms, almost half (~45%) of the nitrate profiles came from Stn. S3. The use of data from a single station could bias the algorithms. However, our tests of validity of the algorithms with independent data from wider locations showed good performance (Fig. 5). The comparison between *in situ* and estimated nitrate profiles in different seasons (Figs. 6A-D) clearly showed the seasonal variation of nitrate profile particularly in ML and IML as a result of seasonal evolution of the MLD, with maximum and minimum in winter and summer, respectively. In winter, the decreasing SST causes deepening of MLD and results in highest and homogeneous nitrate throughout the ML (Fig. 6A). On the other hand, during summer, the sea surface heating in combination with phytoplankton productivity prevailing physical mixing results in very shallow MLD with lower nitrate (Fig. 6C) compared to spring (Fig. 6B) and fall (Fig. 6D).

Since the algorithms of this study had been developed based on general water mass characteristics within the upper 200m of the Sagami Bay, it may be difficult to apply the algorithm when the water is affected by un-identified water masses of different nitrate concentrations, especially in the near-shore stations. Even with this limitation, the fact that DL in ~130-200m depth of Sagami Bay showed stable T-S-nitrate relationship made us confidence that our algorithms can provide valid estimates of nitrate input from deeper layer coused by wind-induced upwelling and/or topographic effect on Kuroshio current.

We are not certain whether our approach could be directly applicable to other embayments, nevertheless this study suggests that a similar approach could be applicable to reconstruct high resolution nitrate profiles that could be used for studying daily, seasonal to annual changes based on temperature, Chl *a* and salinity from automated instruments commonly used on various oceanographic monitoring platforms, such as floats, gliders and buoys.

5. Conclusions

Algorithms for nitrate, constructed using physical (temperature, salinity) and biological (Chl *a*) data from different water masses in different seasons, were able to yield highly reliable, high-resolution profiles of nitrate in upper 200 m water column of the Sagami Bay. The water mass analysis using T-S diagram and MLD as a criteria to distinguish between water masses, yielded a better basis and understanding of the controlling factors of nitrate

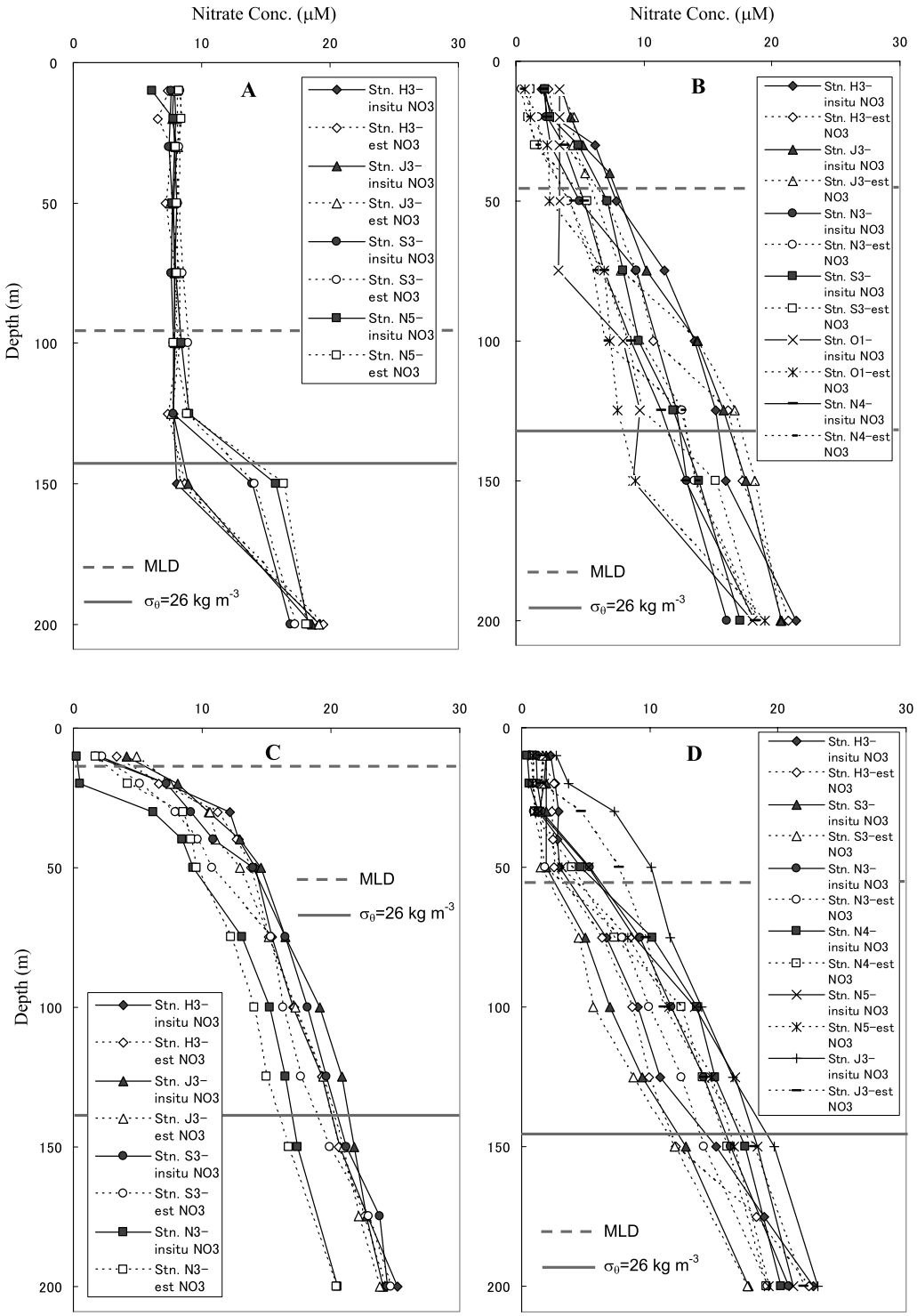

Fig. 6. Comparisons of measured and estimated nitrate profiles in Sagami Bay in winter (A), spring (B), summer (C) and fall (D).

variability in the bay. The analysis helped isolate ML from the DL which had distinct water properties (low temperature, high salinity and nitrate) compared to the IML or the ML.

Previous studies have demonstrated the possibility of nitrate estimation in the MLD derived from temperature (KAMYKOWSKI, 1987; GARSIDE and GARSIDE, 1995; CHAVEZ *et al.*, 1996; SWITZER *et al.*, 2003; HENSON *et al.*, 2003; SHERLOCK *et al.*, 2007). It may be noted that deriving nitrate based on temperature alone is limited because of the highly variable nature of nitrate over space and time (GOES *et al.*, 1999; 2000). Our study suggests that nitrate algorithms based on temperature, salinity and Chl *a* which take into account the water mass characteristics of a given area could be a better and a more robust approach estimating nitrate concentrations in water column even in highly dynamic coastal environments.

This study also demonstrates that these algorithms could be reliably used to fill in the gaps of in situ measurements of nitrate concentration, such data are difficult to obtain by conventional means, such as from research vessels, or another platform, for instance: floats, gliders, and buoys. This study is the first effort to demonstrate the advantages of utilizing a combination of biological and physical parameters for obtaining high resolution nitrate, profiles which could be important for better understanding of carbon fluxes and biogeochemical processes in coastal-oceanic waters.

Acknowledgment

We acknowledge the captains and crew members of *R/V* Tansei-maru, JAMSTEC, for their help in collecting samples in the Sagami Bay. We thank the Japan Oceanographic Data Center, for providing oceanographic data. We express our gratitude to Drs. Joaquim I. GOES and Helga R. GOMES of Bigelow Laboratory for Ocean Sciences, Maine, USA, for the helpful discussions and critical reading of the manuscript. Also to Drs. Y. MINO, Sandric LEONG, Eko SISWANTO and Takuji HOSAKA of Nagoya University, for their helpful suggestions throughout this work and various cruises. A PhD fellowship award of the International Priority Graduate Programs (PGP) from the Japanese Ministry of Education, Culture, Sports, Science and Technology (MEXT) to first author is gratefully acknowledged.

References

ATKINSON, L. P., J. O. BLANTON, C. MCCLAIN, T. N. LEE, M. TAKAHASHI, T. ISHIMARU, and J. ISHIZAKA (1982): Observations of upwelling around the Izu Peninsula, Japan. J. Oceanogr. Soc. Japan, **43**, 89–103.

ARRIGO, K. (2005): Marine microorganisms and global nutrient cycles. Nature, **437**. 349–355.

BAEK, S. H., S. SHIMODE, H. KIM, M. S. HAN, and T. KIKUCHI (2009): Strong bottom-up effects on phytoplankton community caused by a rainfall during spring and summer in Sagami Bay, Japan. Journal of Marine Systems, **75**, 253–264.

CHAVEZ, F., S. SERVICE and S. BUTTREY (1996): Temperature-nitrate relationships in the central and eastern tropical Pacific. J. Geophys. Res., **101** (C9), 20553–20563.

DUGDALE, R.C. and J.J. GOERING (1967): Uptake of new and regenerated forms of nitrogen in new production. Limnol. Oceanogr., **12**, 196–206.

FANNING, K. (1989): Influence of atmospheric pollution on nutrient limitation in the ocean. Nature, **339**, 460–463.

GARSIDE, C., and J. C. GARSIDE (1995): Euphotic zone nutrient algorithms for the NABE and EqPac study sites. Deep-Sea Res., Part II, **42** (2–3), 335–347.

GARSIDE, C., J. C. GARSIDE, M. D. KELLER and M. E. SIERACKI (1996): The Formation of High Nutrient-Low Salinity Water in the Gulf of Maine: a Nutrient Trap?. Estuarine, Coastal and Shelf Science. **42**, 617–628

GOES, J., T. SAINO, H. OAKU, and D. L. JIANG (1999): A method for estimating sea surface nitrate concentrations from remotely sensed sea surface temperature and chlorophyll a－A case study for the North Pacific Ocean using OCTS/ADEOS data, IEEE Trans. Geosci. Remote Sens., **37**, 1633–1644.

GOES, J., T. SAINO, H. OAKU, J. ISHIZAKA, C. S. WONG, and Y. NOJIRI (2000): Basin scale esimates of sea surface nitrate and new production from remotely sensed sea surface temperature and chlorophyll. Geophys. Res. Lett., **27**, 1263–1266.

GONG, G.C., K.K. LIU, and S.C. PAI (1995): Prediction of nitrate concentration from two end member mixing in the southern East China Sea. Cont. Shelf Res., **15**, 827–842.

HASHIMOTO, S., N. HORIMOTO, Y. YAMAGUCHI, T. ISHIMARU and T. SAINO (2005): Relationship between net and gross primary production in the Sagami Bay, Japan. Limnol Oceanogr., **50**: 1830–

1835.

HASHIMOTO, S., N. HORIMOTO, T. ISHIMARU and T. SAINO (2006): Metabolic balance of gross primary production and community respiration in Sagami Bay, Japan. Mar Ecol Prog Ser., **321**: 31–40.

HENSON, S., R. SANDERS, J. ALLEN, and I. ROBINSON (2003): Seasonal constraints on the estimation of new production from space using temperature-nitrate relationships. Geophys. Res. Lett., **30**, 1912, doi:10.1029/2003GL017982.

HINATA, H., T. YANAGI, T. TAKAO, and H. KAWAMURA (2005): Wind-induced Kuroshio warm water intrusion into Sagami Bay. J. Geophys. Res., **110**, C03023, doi:10.1029/2004JC002300.

ISHIZAKA, J., M. TAKAHASHI, and S. ICHIMURA (1983): Evaluation of coastal upwelling effects on phytoplankton growth by simulated culture experiments. Mar. Biol., **76**, 271–278.

ISHIZAKA, J., H. FUKUSHIMA, M. KISHINO, T. SAINO, and M. TAKAHASHI (1992): Phytoplankton Pigment Distributions in Regional Upwelling around the Izu Peninsula Detected by Coastal Zone Color Scanner on May 1982. J. Oceanogr., **48**, 305–327.

ISHIZAKA, J., E. SISWANTO, T. ITOH, H. MURAKAMI, Y. YAMAGUCHI, N. HORIMOTO, T. ISHIMARU, S. HASHIMOTO and T. SAINO (2007):Verification of Vertically Generalized Production Model and Estimation of Primary Production in Sagami Bay, Japan. J. Oceanogr., **64**, 517–524.

IWATA, S (1985): Physics, p.p. 401–409. *In* Coastal Oceanography of Japanese Islands, ed. by Coastal Oceanography Research Committee. The Oceanographical Society of Japan, Tokai University Press, Tokyo. 1106 pp.

IWATA, T., Y. SHINOMURA, Y. NATORI, Y. IGARASHI, R. SOHRIN and Y. SUZUKI (2005): Relationship between Salinity and Nutrients in the Subsurface Layer in the Suruga Bay. J. Oceanogr., **61**, 721–732.

JOHNSON, K. S., L. J. COLETTI, and F.P. CHAVEZ (2006): Diel nitrate cycles observed with in situ sensors predict monthly and annual new production. Deep-Sea Res I, **53**, 561–573.

KAMATANI, A., N. OGURA, N. NAKAMOTO, M. FUNAKOSHI, and S. IWATA (1981): Distribution of nutrients in Sagami Bay during 1971-1973. Bulletin of the Japanese Society of Scientific Fisheries, **47**, 1493–1498.

KAMYKOWSKI, D (1987): A preliminary biophysical model of the relationship between temperature and plant nutrients in the upper ocean. Deep-Sea Res., **34**, 1067–1079.

KAMYKOWSKI, D. and S. J. ZENTARA (1986): Predicting plant nutrient concentrations from temperature and sigma-t in the world ocean. Deep-Sea Res., **33**, 89–105.

KAMYKOWSKI, D., S.J. ZENTARA, J.M. MORRISON, and A.C. SWITZER (2002): Dynamic global patterns of nitrate, phosphate, silicate, and iron availability and phytoplankton community composition from remote sensing data. Global Biogeochemical Cycles, **16**, 1077–1094.

KANDA, J., S. FUJIWARA, H. KITAZATO, and Y. OKADA (2003): Seasonal and annual variation in the primary production regime in the central part of Sagami Bay. Prog. Oceanogr., **57**, 17–29.

LEVITUS, S. (1982): Climatological Atlas of the World Ocean, NOAA Professional Paper 13., U.S. Govt. Print Office.

LEVITUS, S., M. CONKRIGHT, J. REID, R. NAJJAR, and A. MANTYLA (1993): Distribution of nitrate, phosphate and silicate in the world oceans. Prog. Oceanogr., **31**, 245–273.

MARRA, J., R. R. BIDIGARE, and T. D. DICKEY (1990): Nutrients and mixing, chlorophyll and phytoplankton growth, Deep-Sea Res., **37**, 127–143.

OTOBE, H and T. ASAI (1985): The balance of the upper ocean under a land and sea breez in Sagami Bay in summer. Journal of the Oceanographical Society of Japan. **41**, 299–306.

PARSONS, T., M. TAKAHASHI, and B. HARGRAVE (1977): Biological Oceanographic Processes. Elsevier, New York, 330 pp.

PRICE, J. F., R. A. WELLER, and R. PINKEL (1986): Diurnal Cycling: Observations and Models of the Upper Ocean Response to Diurnal Heating, Cooling, and Wind Mixing. J. Geophys. Res., **91** (C7), 8411–8427.

SENJYU, T., N. ASANO, M. MATSUYAMA and T. ISHIMARU (1998): Intrusion Events of the Intermediate Oyashio Water into Sagami Bay. Japan, J. Oceanogr., **54**, 29–44.

SHERLOCK, V., S. PICKMERE, K. CURRIE, M. HADFIELD, S. NODDER, and P. W. BOYD (2007): Predictive accuracy of temperature-nitrate relationships for the oceanic mixed layer of the New Zealand region. J. Geophys. Res., **112**, C06010, doi:10.1029/2006JC003562.

SILIÓ-CALZADA, A., A. BRICAUD, and B. GENTILI (2008): Estimates of sea surface nitrate concentrations from sea surface temperature and chlorophyll concentration in upwelling areas: A case study for the Benguela system. Remote Sensing of Environment, **112**, 3173–3180.

STEINHOFF, T., T. FRIEDRICH, S. E. HARTMAN, A. OSCHLIES, D. W. R. WALLACE, and A. KORTZINGER (2009): Estimating mixed layer nitrate in the North Atlantic Ocean. Biogeosciences Discuss., **6,** 8851–8881.

SUZUKI, R., and T. ISHIMARU (1990): An improved method for the determination of phytoplankton

chlorophyll using N,N-dimethylformamide. J. Oceanogr. Soc. Japan., **46**, 190–194.

SWITZER, A., D. KAMYKOWSKI, and S. J. ZENTARA (2003): Mapping nitrate in the global ocean using remotely sensed sea surface temperature. J. Geophys. Res., **108** (C8), 3280. doi:10.1029/2000 JC000444.

TAKAHASHI, M., I. KOIKE, T. ISHIMARU, T. SAINO, K. FURUYA, Y. FUJITA, A. HATTORI, and S. ICHIMURA (1980): Upwelling Plumes in Sagami Bay and Adjacent Water around the Izu Islands, Japan. J. Oceanogr. Soc. Japan, **36** (4). 209–216.

TAKAHASHI, M., J. ISHIZAKA, T. ISHIMARU, L.P. ATKINSON, T.N. LEE, Y. YAMAGUCHI, Y. FUJITA and S. ICHIMURA (1986): Temporal change in nutrient concentrations and phytoplankton biomass in short time scale local upwelling around the Izu Peninsula. Japan, J. Plank. Res., **8**. 1039–1049.

WELSCHMEYER, N. A. (1994): Fluorometric analysis of chlorophyll a in the presence of chlorophyll b and pheopigments, Limnol. Oceanogr., **39** (8), 1985–1992.

YANAGI, T., and H. HINATA (2004): Water exchange between Tokyo Bay and the Pacific Ocean during winter. Ocean Dynamics, **54**: 452–459.

Received: January 28, 2010
Accepted: May 25, 2010